Study of the ferroelectric phase transition in germanium telluride using time-domain terahertz spectroscopy

Filip Kadlec, Christelle Kadlec, Petr Kužel, and Jan Petzelt
Institute of Physics, Academy of Sciences of the Czech Republic, Na Slovance 2, 182 21 Prague 8, Czech Republic
(Received 8 August 2011; published 14 November 2011)

Germanium telluride (GeTe) is a ferroelectric material presenting, at room temperature, both spontaneous polarization and electrical conductivity. Despite the simplicity of its crystal structure, the mechanism of the phase transition is still not well understood; the free charge carriers prevent the use of traditional spectroscopic techniques which could provide detailed information. While, for a long time, the transition was believed to be of displacive character, recent evidence suggests an order-disorder type. We report results of high-temperature measurements of GeTe thin films by means of terahertz spectroscopy showing the absence of critical phonon softening and revealing a low-frequency excitation in the paraelectric phase. We suggest two possible mechanisms which could be at the origin of this feature: either a critical relaxation related to the phase transition or hopping of free charge carriers. The former mechanism appears more probable due to the observed temperature evolution of the spectra. This indicates a mixed character of the phase transition; assuming a Curie-Weiss behavior, we deduce the value of the Curie-Weiss constant as $C \approx 1 \times 10^5$ K.

DOI: 10.1103/PhysRevB.84.205209 PACS number(s): 77.80.B−, 72.20.−i, 77.55.−g, 78.30.−j

I. INTRODUCTION

Germanium telluride (GeTe) is a material presenting a particular interest from various points of view. It is a narrow-gap semiconductor belonging to the class of so-called phase-change materials; its conducting properties, as well as those of the related chalcogenide alloys $Ge_xSb_yTe_z$, have been intensely studied, since these materials are regarded as very promising candidates for use in nonvolatile memory applications and for DVD disk optical data storage.[1,2] Recently, novel advanced concepts of electronics, namely, nanoscale electronic synapses[3] and an optical arithmetic processor[4] based on $Ge_2Sb_2Te_2$ were demonstrated. Similarly to the ternary compounds, thin films of GeTe can also be deposited in an amorphous state which displays a contrast of several orders of magnitude in electrical conductivity as compared to the crystalline state. At the same time, as a compound with only two types of atoms in the unit cell, GeTe is the simplest known ferroelectric.[5] Despite this, there is still a controversy about the character of the ferroelectric (FE) phase transition (PT) in GeTe; the experimental studies have been hindered by its high conductivity, which is a rare feature among ferroelectrics.

The ferroelectric phase transition separates the rhombohedral α phase, occurring at room temperature, from the high-temperature cubic β phase with the rocksalt structure where the material is paraelectric (PE). The values of the critical temperature were reported to be $T_c = 705$ K (Ref. 6) and 625 K (Ref. 7) for single crystals and $T_c = 553$ K for thin films.[8] From neutron diffraction, it was possible to determine the temperature dependence of the lattice parameter and of the rhombohedral angle of the unit cell.[6] In Raman scattering measurements, the A_1- and E-symmetry phonon modes were observed in the ferroelectric phase; they were found to decrease their frequencies as T_c is approached.[7] These findings supported the idea of the displacive character of the phase transition accepted later by other authors.[9] At the same time, Raman scattering is, in principle, unable to provide information about mode softening in the β phase; while the two modes observed in the α phase are Raman and infrared (IR) active, in the β phase they merge into a triply degenerate F_{1u} mode which is Raman inactive and IR active.[7] Also, a partial softening of the A_1 mode from 3.8 THz down to 2.5 THz was observed upon coherent phonon excitation by a train of femtosecond optical pulses at a terahertz rate.[10]

Recently, high-temperature extended x-ray absorption fine structure (EXAFS) and x-ray absorption near-edge structure (XANES) measurements[11] have shown that the Ge-Te bond length does not display an anomaly around T_c. This raised questions about the displacive character of the phase transition and led the authors to the statement that the transition is of order-disorder type. Although, in principle, the traditional approach consisting in dividing the ferroelectric phase transitions between order-disorder and displacive types may fail as various compounds simultaneously exhibit features characteristic of both types,[12,13] the question about the predominant character of the phase transition in GeTe is of fundamental interest. Therefore, new experimental studies especially of the low-frequency excitations appear to be worthwhile.

The usual kilohertz to megahertz range measurements of the dielectric anomaly in GeTe have not, to our knowledge, been performed, which is clearly linked to the semiconducting nature of the crystal and to its relatively high dc conductivity. However, anomalies of the static dielectric constant were observed[14] in the isostructural crystals of $Pb_{1-x}Ge_xTe$ with $x \leqslant 0.05$, where the ferroelectric PT occurs at temperatures below 100 K and increases with x. Similarly, there are no reports of GeTe phonon measurements by means of IR spectroscopy; also here, a consequence of the interaction of IR radiation with free carriers is the high reflectance and opacity of the bulk crystals which make such studies difficult to realize.

Time-domain terahertz (THz) spectroscopy, where time-domain wave forms of the transmitted electric field amplitude $E(t)$ are detected, is an alternative method convenient for studying the polar excitations in the far IR. Compared to the standard Fourier-transform IR spectroscopy, its advantage is the possibility to measure the phase of the transmitted

radiation and thus determine the complex spectra of optical constants without assuming their particular form. Also, its sensitivity at long wavelengths is higher, and, owing to the use of ultrashort broadband THz pulses and a gated detection technique, the measurements at high temperatures do not suffer from problems linked to the continuous thermal radiation. For these reasons, time-domain THz spectroscopy appears as an ideal tool for studying the polar excitations related to the GeTe phase transition, provided that thin film samples are used. In this paper we present a temperature-dependent study of the GeTe optical constants which reveals a previously unreported (to our knowledge) low-frequency relaxation supporting the order-disorder character of the phase transition. As we show below, the high-temperature measurements of these thin films are not a routine task because the highest possible measurement accuracy is required and special care has to be taken in every step of the procedure.

II. SAMPLES AND EXPERIMENTAL DETAILS

Amorphous thin films of GeTe with a nominal thickness of 500 nm were deposited by means of magnetron sputtering on fused silica glass substrates, which are transparent to THz radiation, with dimensions of about $10 \times 7.5 \times 1$ mm^3. Their crystallization was achieved by subsequent annealing at 300 °C. In order to avoid changes of their chemical compositions, the films were covered by a 30-nm-thick $(ZnS)_{80}(SiO_2)_{20}$ capping layer. For two different samples, the capping layer was deposited either immediately after the GeTe deposition (*in situ*) or after annealing (*ex situ*). While the first approach ensures the lowest possible pollution of the sample surface, the second one presents *a priori* the advantage of reducing the strain between the layers, since the crystallization induces a change of the layer density by several percent.

We employed a custom-made experimental setup for time-domain THz spectroscopy based on a Ti:sapphire laser oscillator (Coherent Mira) providing pulses with a central wavelength of 810 nm and duration of 80 fs at a 76 MHz repetition rate. The pulses excited an interdigitated photoconducting emitter[15] generating linearly polarized THz pulses. A weak part of the laser beam was directed on a 1-mm-thick ⟨110⟩-cut ZnTe crystal for electro-optic sampling of the transmitted THz waves, leading to a useful spectral range of 0.25–2.5 THz. The samples were placed in a furnace with optical ports, using a clear aperture of 6 mm, and heated to a temperature of up to 450 °C. The furnace and the whole THz beam were enclosed in a rough vacuum chamber (about 20 mbar pressure) in order to avoid water vapor absorption. The measurements were performed first on heating, with a step of 50 or 25 °C, and after the maximum temperature was reached, also on cooling. Since the furnace features only one sample holder, it was not possible to perform reference measurements after each temperature change, as is usual in room- or low-temperature experiments. Therefore, just before and after the temperature run, we carried out room-temperature reference measurements with a bare fused silica substrate of a thickness $d_r \approx 1$ mm. In this way, slight changes of amplitude due to instrument instability (about 3% after 6 h) were detected and later compensated for by a linear time-dependent interpolation.

For an optimal evaluation of the optical constants of the films, special care was taken in the substrate choice and characterization. This is necessary because the optical thickness of the film is much lower than that of the substrate; while the detection method is phase sensitive, it is not possible to differentiate the phase delay acquired during the propagation through the film from that acquired in the substrate. Therefore, a small relative error in the knowledge of the substrate thickness can bring a very high error in the spectra of the optical constants of the films;[16] see also below for details. The thickness of the films ($d = 480 \pm 20$ nm) was determined by means of a surface profiler; the thickness d_s and plane parallelism of the substrates were carefully measured by a linear displacement gauge with a ± 1 μm precision. Finally, the values of $d_s(T)$ used for the thicknesses of the fused silica substrates were optimized with a submicrometer precision using the first Fabry-Perot-like echo of the pulse[17] in the wave forms transmitted through the substrates, $E_r(t)$. With this aim, before the film deposition, we measured the temperature dependence of the substrate transmittance and determined the variation of their thickness and refractive index with temperature. Within all data treatments, we also took into account the correction related to the Gouy phase shift of the focused probe beam.[18]

III. RESULTS AND EVALUATION

Although we performed several heating runs, we did not detect, within the available precision, any temperature-dependent hysteresis effects. Also, the measured spectra of the two samples with the capping layers deposited *in situ* and *ex situ* were the same, within the available precision. The *in situ*–capped sample displayed a discontinuity in the spectral evolution, corresponding most likely to changes of GeTe chemical composition, starting from 500 °C. The data presented below correspond to the *ex situ*–capped sample, the spectra of which were the same before the heating run and after it.

The extraction of complex permittivity spectra of the sample as a function of temperature required several steps. Using the usual procedure including measurement of the reference signal with no sample $E_0(t)$, the spectrum of the refractive index of the fused silica substrates as a function of angular frequency, $N_s(\omega)$, was determined before the film deposition, as well as its temperature dependence. The influence of the capping layers on the THz field $E_f(t)$ transmitted through the films on substrates was neglected based on the fact that their optical thickness is much smaller than that of the films.

The spectra of the complex refractive index of GeTe films, $N(\omega) \equiv n + i\kappa$, were determined by numerically inverting the expression[19] for complex transmittance, $t(\omega) \equiv E_f(t)/E_r(t)$:

$$t(\omega) = \frac{2N(N_s+1)\,e^{i\omega(N-1)d/c}e^{i\omega(N_s-1)(d_s-d_r)/c}}{(1+N)(N+N_s)+(1-N)(N-N_s)e^{i\omega 2Nd/c}}, \tag{1}$$

where c denotes the the light speed in vacuum. The refractive index spectra for three selected temperatures are shown in Fig. 1; they feature a prominent rise toward the low frequencies, which is a clear sign of metal-like properties. From the refractive index, the complex permittivity spectra

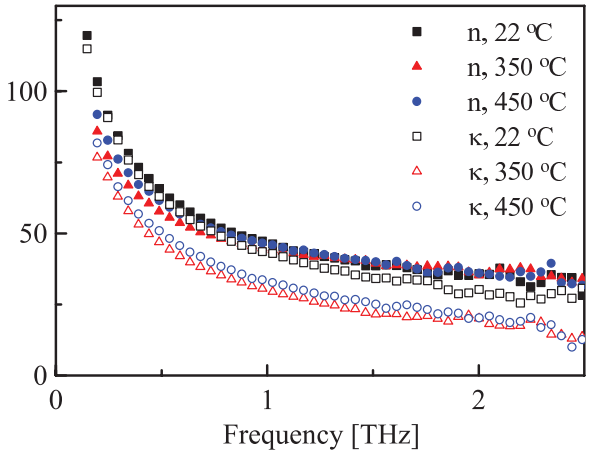

FIG. 1. (Color online) THz spectra of the complex refractive index of GeTe calculated from experimental data using Eq. (1).

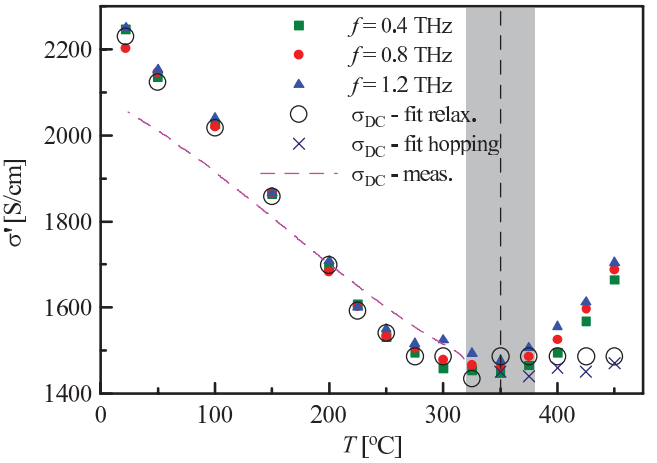

FIG. 2. (Color online) Full symbols: temperature dependence of the conductivity at selected frequencies, displaying a minimum at 350 °C, corresponding to the PT. Open symbols: values of dc conductivity obtained from fitting the THz spectra by Eqs. (5) and (6). Crosses: fit by Eq. (7). Dashed line: dc conductivity measured by the Van der Pauw method on a 75-nm-thick GeTe film. The gray zone indicates the estimated uncertainty in determining T_c.

were then calculated as $\hat{\varepsilon} \equiv \varepsilon' + i\varepsilon'' = N^2$, i.e., $\varepsilon' = n^2 - \kappa^2$, $\varepsilon'' = 2n\kappa$.

Despite all the precautions taken, there is still a small systematic error in both the real and imaginary parts of N. This error may appear due to remaining uncertainties in determination of the thickness of both the substrates and films, possible slight deviations of the parallelism of their surfaces, and also because of instability of the experimental setup in time; in particular, the furnace heating may lead to small temperature increase of elements in the THz beam path leading, e.g., to deformations on the scale of a few micrometers. Upon solving Eq. (1), the above-mentioned small systematic errors then transform into uncertainties in the calculated spectra of $N(\omega)$. We estimate the absolute errors in both n and κ to be of the order of unity. At the same time, as one can see from Fig. 1, the spectra of the real and imaginary parts of the refractive index have very similar shapes. It appears that for such shapes of the spectra, any slight change of film thickness d, of the substrate optical thickness $N_s d_s$, or of complex transmittance will lead to an increase of the real part n and decrease of the imaginary part κ or vice versa. If we denote these variations by Δn and $\Delta\kappa$, respectively, the calculated real part of the permittivity reads

$$\varepsilon' \equiv (n + \Delta n)^2 - (\kappa + \Delta\kappa)^2 = n^2 - \kappa^2 + 2n\Delta n - 2\kappa\Delta\kappa, \tag{2}$$

where the higher-order terms were omitted. Since the signs of Δn and $\Delta\kappa$ are opposite, the deviation terms add up and amount to values comparable to the actual value of the permittivity; as n and κ attain values of several tens, the resulting error in ε' is of the order of hundreds. However, Δn and $\Delta\kappa$ are frequency dependent, and from the numerical solution of Eq. (1) it appears that the resulting error is virtually constant as a function of frequency, i.e., it manifests itself as an offset of the whole $\varepsilon'(\omega)$ curves. We conclude that the shapes of the $\varepsilon'(\omega)$ spectra appear to be correct except for this frequency-independent offset.

By contrast, in the imaginary part spectra, both the relative and absolute errors $\varepsilon''(\omega)$ are substantially lower. Accounting for the errors in N, we may write

$$\varepsilon'' \equiv 2(n + \Delta n)(\kappa + \Delta\kappa) = 2n\kappa + 2n\Delta\kappa + 2\kappa\Delta n. \tag{3}$$

Here the error terms are much smaller than the leading one, and, moreover, they will cancel out to a large extent owing to their opposite signs. Consequently, the imaginary part spectra can be determined with a much better precision than those of the real part; we estimate the error to be on the order of tens.

For any fixed frequency, the calculated values of $\sigma'(\omega)$ exhibit a temperature dependence with a flat minimum at $T = 350\,^{\circ}\mathrm{C}$, which appears to correspond to the PT temperature. This is illustrated in Fig. 2 for three different values of frequencies; we assume that the phase transition occurs at this minimum, $T_c \approx 350 \pm 30\,^{\circ}\mathrm{C}$. Our value corresponds exactly to that determined by differential thermal and x-ray studies in Ref. 7 and lies between those reported from x-ray and neutron diffraction experiments in Refs. 6 and 8. Furthermore, it is also confirmed by our detailed data analysis presented below, showing a change of dynamics near this temperature.

IV. MODELING AND DISCUSSION

In the low-frequency part, the spectra of the imaginary part of permittivity exhibit a marked rise $\propto 1/\omega$, in accord with the Drude theory. Therefore, for the purpose of spectral modeling, we converted them according to the known identity $\hat{\varepsilon}(\omega) \equiv \frac{i\sigma}{\varepsilon_0\omega}$ to real conductivity $\sigma'(\omega) = \varepsilon_0\omega\varepsilon''(\omega)$ where ε_0 is the vacuum permittivity. Subsequently we sought a model able to fit the real parts of the permittivity and conductivity spectra at all temperatures.

A. FE phase

In the FE phase, the experimentally obtained spectra of both $\sigma'(\omega)$ and $\varepsilon'(\omega)$ are close to a constant. Our model

of dielectric function involves the response of free carriers, and we know from previous studies that it must also include an oscillator term describing the phonon mode observed by Raman spectroscopy.[7] The simplest expression then reads

$$\hat{\varepsilon}_{\mathrm{FE}}(\omega) = \varepsilon_\infty + \frac{\Delta\varepsilon\omega_0^2}{\omega_0^2 - \omega^2 - i\omega\Gamma} - \frac{\omega_\mathrm{p}^2}{\omega^2 - i\omega\gamma}, \qquad (4)$$

where ε_∞ denotes the high-frequency limit of permittivity, ω_0 and ω_p are the oscillator eigenfrequency and free-carrier plasma frequency, respectively, Γ denotes the oscillator damping, γ is the carrier scattering rate, and $\Delta\varepsilon$ is the contribution of the oscillator to $\varepsilon'(\omega)$.

We fitted simultaneously all spectra of real $\varepsilon'(\omega)$ and $\sigma'(\omega)$ parts at all measured temperatures. The (temperature-dependent) constant ε_∞ not only includes the terms lying above the THz range, but, as mentioned above, mainly accounts for the systematic error[16] stemming from a limited precision in measuring d_s.

For the plasma frequency, one may also write $\omega_\mathrm{p}^2 = N_\mathrm{c}e_0^2/m\varepsilon_0$, where N_c, m, and e_0 denote the free-carrier concentration, effective mass, and elementary charge, respectively. Although the contribution of the free charge carriers can be identified very clearly through the low-frequency increase of the complex refractive index (see Fig. 1), the THz spectra provide only limited information about the free-carrier plasma. This appears to be a more general feature of the phase-change materials where the momentum scattering time typically amounts to a few femtoseconds only,[20] the carrier concentration is of the order of 10^{20} cm^{-3}, and the plasma frequency lies well beyond the THz range. Therefore, the Drude term contribution to the THz conductivity is flat, and of the two parameters entering into the model (carrier concentration, scattering rate) it is not possible to determine both. By contrast, our procedure enables us to evaluate quite precisely the extrapolated static conductivity, which is proportional to their ratio, $\sigma_\mathrm{dc} = N_\mathrm{c}e_0^2/(m\gamma)$ and, in the FE phase, it corresponds directly to the level of our $\sigma'(\omega)$ spectra. Therefore, Eq. (4) can be written more simply in the form

$$\hat{\varepsilon}_{\mathrm{FE}}(\omega) = \varepsilon_\infty + \frac{\Delta\varepsilon\omega_0^2}{\omega_0^2 - \omega^2 - i\omega\Gamma} + \frac{i\sigma_\mathrm{dc}}{\varepsilon_0\omega}, \qquad (5)$$

which was used for the fitting.

The oscillator frequencies were fixed during the fitting; in the FE phase, we set the frequencies $\omega_0(T)$ to values corresponding to those determined previously by Raman measurements[7,11] (see Fig. 3). Note, however, that these works report values of T_c different from the one we detect in our thin film sample, so instead of employing the same values of ω_0 at the given T, we determined the expected values relative to the reported phase transition temperatures, i.e., for the same temperature offsets $(T - T_\mathrm{c})$. Given the relatively high values of the oscillator damping, a shift of ω_0 by a few percent has very little influence on the shape of the spectra.

The agreement of our fits with the experimental data is good, taking into account that our experimental data are somewhat noisy above 1.6 THz (see Fig. 4). Although the phonon cannot be clearly discerned in the measured spectra, our fitting results show that the oscillator strength cannot be substantially higher than our resulting value and that the

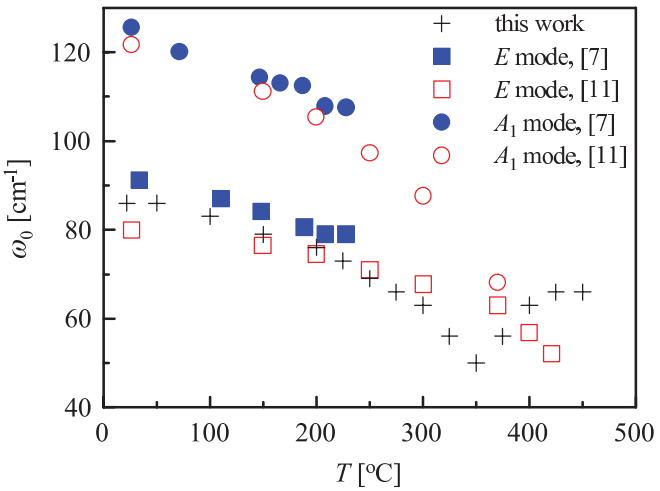

FIG. 3. (Color online) Temperature dependence of the oscillator eigenfrequency (describing the E-symmetry phonon) used in the model of $\hat{\varepsilon}(\omega)$ compared to values determined by Raman measurements on bulk crystals (Ref. 7) and thin films (Ref. 11).

mode softening stops approximately near 1.5 THz; see also the discussion in the following section. The values of extrapolated static conductivity $\sigma_\mathrm{dc}(T)$ obtained from the fits are plotted by open circles in Fig. 2. For comparison, data measured by the Van der Pauw method on a thinner sample (about 75 nm) with a slightly different thermal history are shown by the dashed line. Both sets of data display the same decreasing tendency upon heating, and their values are in a good agreement within the estimated precision.

B. PE phase: Hypothesis of a relaxation mode

The experimental data obtained in the PE phase are clearly different from those of the FE phase, since a marked curvature develops in the low-frequency part of the spectra upon heating (see Fig. 5). This feature is the most pronounced at the highest temperature measured, $T = 450\,^\circ$C. In view of the open debate about the character of the PT, it appears natural to include a supplementary term into the model, namely, a relaxation mode.

The model for the dielectric function can then be written as

$$\hat{\varepsilon}_{\mathrm{PE}}(\omega) = \hat{\varepsilon}_{\mathrm{FE}}(\omega) + \frac{\Delta\varepsilon_\mathrm{r}\omega_\mathrm{r}}{\omega_\mathrm{r} - i\omega}, \qquad (6)$$

where $\Delta\varepsilon_\mathrm{r}$ is the contribution of the relaxation mode to $\varepsilon'(\omega)$ and ω_r denotes its eigenfrequency. The additional term is justified by the characteristic shapes of the spectra which cannot be described by an oscillatory term. This can be seen very clearly from the values of the real part of permittivity near the lower limit of our frequency range [see Fig. 5(a)], which rise and develop a convex shape as temperature increases. From the temperature series, it is evident that if a relaxation mode is responsible for the low-frequency behavior of $\varepsilon'(\omega)$ and ω_r, then the frequency ω_r must lie below the THz range or at its lower limit. For this reason, the relaxation mode parameters can, in principle, be chosen in different ways.

Without further assumptions, the data from the THz spectral region do not allow us to make any conclusions about the origin of this spectral feature. The natural choice, which we discuss below, is based on the hypothesis of a critical relaxation leading

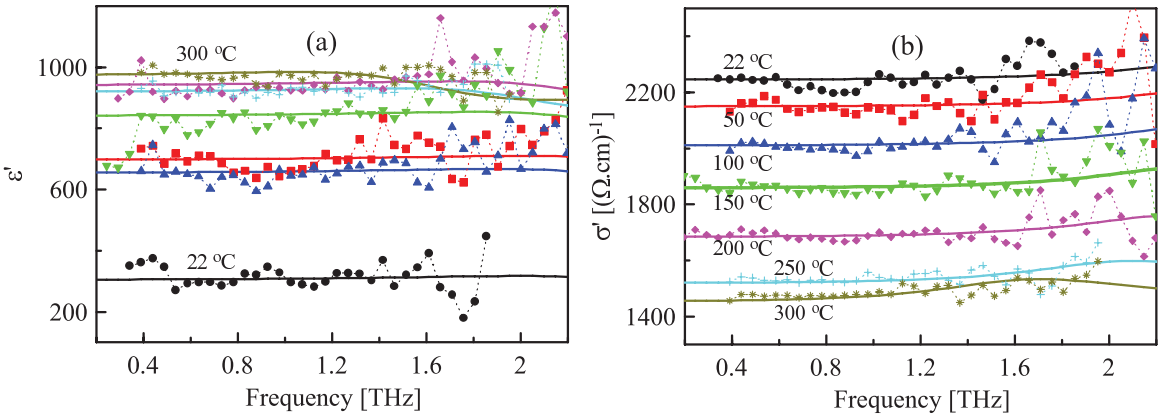

FIG. 4. (Color online) THz spectra of (a) real permittivity and (b) conductivity of GeTe in the FE phase.

to the PT, known from other order-disorder ferroelectrics. Then, one expects the relaxation frequency to increase linearly as $\omega_r = a(T - T_c)$ and its strength $\Delta\varepsilon_r\omega_r$ to be constant with T; in this case, its contribution $\Delta\varepsilon_r$ to the permittivity satisfies the Curie-Weiss law $\Delta\varepsilon_r = C/(T - T_c)$. We imposed such a behavior on the relaxation mode parameters in the PE phase, and the low-frequency part of the modeled spectra converged well to the experimental data (see Fig. 5). The proportionality constant has then the value of $a = 2.7 \times 10^{-3}$ THz K^{-1} and the Curie-Weiss constant $C \approx (1.0 \pm 0.2) \times 10^5$ K. Within this hypothesis, the THz spectra reveal a high-frequency wing of an overdamped sub-THz mode, which is the dominant driving force of the FE PT. This can be seen from Fig. 6, where the respective contributions of the E phonon mode and the relaxational mode are plotted as functions of temperature. Owing to the assumption of the Curie-Weiss behavior, the relative errors of the relaxational mode strength $\Delta\varepsilon_r$ obtained from the fit are quite small (about 15%), as indicated by the narrower range of error bars for the relaxation mode in Fig. 6.

As for the phonon mode, it is Raman inactive in the PE phase. Consequently, we could not rely on earlier observations to set its eigenfrequency; instead, we assumed the same mode hardening rates with T above and below T_c. Since its contribution to the spectra is not very pronounced, this choice does not have a significant impact on the conclusions of our work.

The curves resulting from modeling based on Eq. (6) are shown in Fig. 5 by solid lines; at all temperatures, they show a very good agreement with the experimental data. Since the features in the spectra due to the phonon are quite broad, it is not possible to determine reliably its damping Γ as a function of T. Therefore, Γ was assumed to be constant within either phase, and by means of fitting, we determined the damping values $\Gamma \approx 40 \pm 10$ cm^{-1} in the FE phase and $\Gamma \approx 80 \pm 20$ cm^{-1} in the PE phase. The same approach was used for the oscillator strength $f = \Delta\varepsilon\omega_0^2$ for which values of $(1.6 \pm 0.2) \times 10^5$ and $(2.4 \pm 0.3) \times 10^5$ cm^{-2} were obtained for the FE and PE phases, respectively.

The shapes of the spectra do not reveal quite clearly the presence of a phonon and we find that the contribution of the soft mode is small in the THz range. Nevertheless, an oscillatory term must be present for compatibility with Raman data, since the two phonons observed in the Raman spectra are also IR active; in particular, the one lying at lower frequencies (E symmetry) lies close to the accessible THz range. Our results show that there is no contradiction among our data, our model, and the previously published Raman data. Owing to this oscillator term, our model can then explain the observed gradual increase of $\sigma'(\omega)$ toward higher frequencies

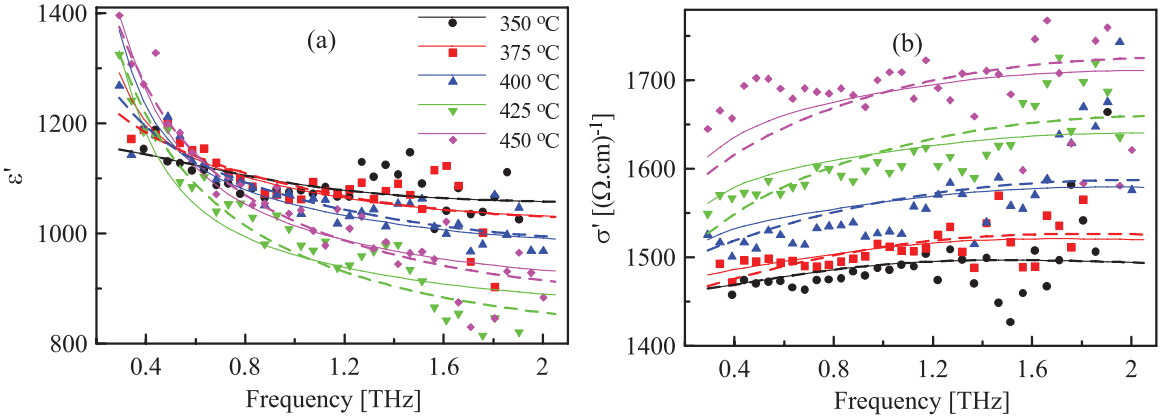

FIG. 5. (Color online) THz spectra of (a) real permittivity and (b) conductivity of GeTe in the PE phase. Symbols: Experimental data. Solid lines: Fits using Eq. (6) including a relaxational mode. Dashed lines: Fits using Eq. (7) based on hopping.

[see Fig. 4(b)]. The values of oscillator damping Γ obtained from our fits are substantially higher than those determined from the Raman measurements; this is apparently linked to the nanocrystalline grains present in the thin film samples, while the Raman spectra[7] were measured on a bulk crystal.

The oscillator strength can be compared to theoretical values previously published in Ref. 21, where the value of the strength tensor for the E mode was predicted as $S_\perp(E) = 56 \times 10^5$ (in atomic units). Taking into account the unit cell volume of about 53 Å^3,[21] this leads to the strength of the E mode of about 2×10^5 cm^{-2} according to the definition in Eq. (4). Our fits yield a value about 20% lower in the FE phase, which can be considered as a good agreement. For the PE phase, we infer from the fits an oscillator strength about 50% higher than the one we determined for the FE phase; this increase is in qualitative agreement with the predicted increase of the Born effective charge.[21] In summary, we can conclude that, even if we do not discern quite clearly the soft mode in the THz spectra, which is apparently due to its high damping, our data are compatible with its existence and our fitting procedure provides parameters corresponding well with the earlier published values. Importantly, our data imply that the phonon mode softening is very limited; should the phonon be the driving factor of the PT then, in the vicinity of T_c, we would necessarily observe a much stronger contribution to our spectra in the lower THz range characterized by a peak in the conductivity and an increased level of the permittivity below ω_0.

Finally, note that the presence of the relaxation mode is the reason why the traces of the symbols in Fig. 2 differ: while the filled ones come from the raw experimental data, the open circles reflect only the dc conductivity owing to the Drude term, and omit the contribution of the relaxation mode.

C. PE phase: Hypothesis of hopping

On the one hand, the fit described above provides a satisfactory description of the observed spectral features and it is in agreement with the recent hypothesis about the order-disorder character of the PT.[11] On the other hand, when the constraints imposed by the Curie-Weiss law are removed, the parameters of the relaxational mode can vary in a much broader range; an estimate of the uncertainty is shown by the wider error bars in Fig. 6; their lower ends correspond to a case when the relaxation frequency would be approximately constant. Therefore, the fit in itself does not provide a sufficient argument to prove unambiguously that the PT is of order-disorder type, and other interpretations of the spectral shapes are possible.

Our samples were annealed from the amorphous phase; they are polycrystalline and, like other phase-change materials, they consist of grains with size of the order of 20 nm.[22] It is known that owing to germanium vacancies, free holes in the valence band play an important role in polycrystalline GeTe.[23] Therefore, in principle, one can envisage that the low-frequency features in the PE phase are related to hopping of carriers captured in states at the grain boundaries. We note that a similar behavior and analogous spectra were observed in microcrystalline and amorphous silicon films,[24] where photocarriers generated by femtosecond pulses were rapidly

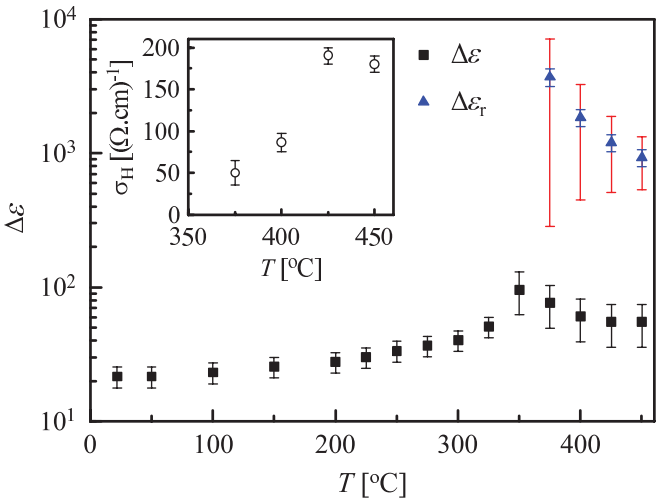

FIG. 6. (Color online) Temperature dependence of the dielectric strengths of the phonon and relaxational modes as obtained from the fit using Eq. (6). For the relaxational mode, the narrower range of error bars is based on the assumption of Curie-Weiss behavior. Inset: temperature dependence of the hopping conductivity σ_H obtained from fitting the spectra in the PE phase with the hopping model [Eq. (7)].

trapped at boundaries of small grains (≈20–30 nm in size). Hopping among these states yields a conductivity dominating the transient spectra of these thin films on the picosecond and subnanosecond time scales.

The data in Ref. 24 were modeled by a hopping model first proposed by Dyre,[25] which assumes an inhomogeneous material with a distribution of barrier energies; the probability of occurrence of all values for these energies is supposed to be the same. Within the hopping hypothesis, we attempted to apply this model to GeTe. We denote by τ_{max} the reciprocal value of Dyre's minimum hopping frequency γ_{min}, i.e., $\tau_{max} \equiv 1/\gamma_{min}$, and analogously $\tau_{min} \equiv 1/\gamma_{max}$. Since we are interested in the high-frequency part of the hopping response, we can assume that $\omega \gg \gamma_{min}$. The corresponding model of the permittivity spectra then includes, instead of the relaxation mode in Eq. (6), a frequency-dependent term due to the hopping:[24]

$$\hat{\varepsilon}_{PE}(\omega) = \hat{\varepsilon}_{FE}(\omega) + \frac{\sigma_H}{\varepsilon_0}\tau_{min}\ln[1 + i/(\omega\tau_{min})], \qquad (7)$$

where σ_H is the contribution of the hopping to the high-frequency conductivity.

Within the fit, we assumed τ_{min} to be temperature independent; this appears reasonable since the nanostructural details of the crystal lattice should not change upon heating. The fit using Eq. (7) then yielded a value of $\tau_{min} = 190 \pm 30$ fs and provided curves very similar to those in the previous case where the relaxation mode was used; the spectra obtained from the fit are shown by the dashed lines in Fig. 5. The values of static conductivity σ_{dc} are shown by the crosses in Fig. 2; they are, for all temperatures, close to 1450 $(\Omega\,\mathrm{cm})^{-1}$.

The inset of Fig. 6 shows the temperature dependence of the hopping conductivity σ_H provided by the fit. While, near $T = T_c$, the value of σ_H cannot be determined since the curvature of the spectra is too small, upon heating, σ_H

progressively increases from about 50 to nearly 200 $(\Omega\,\mathrm{cm})^{-1}$ at $T = 425$ and 450 K. Such a marked rise in a relatively narrow temperature range is most probably not linked to an increase of the hopping carrier mobility; if the hopping hypothesis were true, this would be likely to correspond to an increase of the concentration of hopping carriers. We must note that such a behavior does not correspond to what is usually observed in various systems where hopping conductivity occurs; as a rule, regardless of the hopping model used, the high-frequency conductivity values at different temperatures reach the same limit.[26]

At the same time, a fundamental question arises also about the reason that the hopping appears only above the PT. To the best of our knowledge, there is no analogous case of another system exhibiting such a high electric conductivity and, simultaneously, a FE PT; therefore we can only speculate about the possible origins of these phenomena. It is then natural to assume a link between the strong local electric field due to spontaneous polarization and the absence of hopping in the FE phase. This local field might lead to a suppression of motion among the localized hopping states. By contrast, in the PE phase, this argument by itself seems to fail in explaining the gradual rise of the hopping conductivity σ_H upon heating; one would have to assume precursor effects linked to an onset of the FE ordering upon cooling. At present, we cannot support this hypothesis by additional evidence, and in view of the unusual increase of the high-frequency conductivity with temperature, as discussed in the previous paragraph, it seems to be less probable than that of the relaxation mode.

V. CONCLUSION

In conclusion, we have performed a study of the high-temperature THz spectra of GeTe thin films. We were able to detect the IR activity of its polar excitations; both FE and PE phases were studied. The phase transition occurs at $T_c \approx 350\,^{\circ}\mathrm{C}$, which is in agreement with earlier reported values. We detected at high temperatures an excitation located in the sub-THz range. This mode is absent in the FE phase and unambiguously present in the PE phase; however, the available experimental evidence do not allow us to draw clear conclusions about its microscopic origin.

We have shown that, with respect to this sub-THz mode, the spectra can be interpreted in two ways. First, one can reason in terms of a temperature-dependent critical relaxation mode. Assuming the validity of the Curie-Weiss law, this hypothesis yields a reasonable value of the Curie-Weiss constant of $C \approx 1 \times 10^5$ K. Second, the spectra are equally compatible with a hopping model, the use of which would be justified by the nanocrystalline structure of the films. Unfortunately, since the interplay of FE ordering, high electric conductivity, and nanocrystalline structure represents quite an unusual and complex system, it is not easy to find an unambiguous explanation for the observed behavior without further evidence.

Finally, similarly to what was observed earlier in the Raman spectra, only a limited softening of the lowest-lying phonon is observed; at all temperatures, its eigenfrequency is greater than or equal to 1.5 THz. Therefore, our experimental data, regardless of the interpretation of the low-frequency behavior, appear to provide strong support against the purely displacive type of the PT and indicate rather its mixed nature.

ACKNOWLEDGMENTS

Financial support by the Funding Agency of the Czech Republic (Project No. 202/09/J045) and the Academy of Sciences of the Czech Republic (Project No. AVOZ10100520) is acknowledged. The authors would like to thank P. Jost for growing the samples, providing the results of the Van der Pauw measurements, and extensive discussions, as well as M. Wuttig, S. Kamba, and J. Hlinka for helpful advice.

[1] A. V. Kolobov, P. Fons, A. I. Frenkel, A. L. Ankudinov, J. Tominaga, and T. Uruga, Nat. Mater. **3**, 703 (2004).
[2] M. Wuttig, D. Lüsebrink, D. Wamwangi, W. Welnic, M. Gilleßen, and R. Dronskowski, Nat. Mater. **6**, 122 (2007).
[3] D. Kuzum, R. G. D. Jeyasingh, B. Lee, and H.-S. P. Wong, Nano Lett., doi: 10.1021/nl201040y (to be published).
[4] C. Wright, Y. Liu, K. Kohary, M. Aziz, and R. Hicken, Adv. Mater. **23**, 3408 (2011).
[5] G. S. Pawley, W. Cochran, R. A. Cowley, and G. Dolling, Phys. Rev. Lett. **17**, 753 (1966).
[6] T. Chattopadhyay, J. Boucherle, and H. Vonschnering, J. Phys. C **20**, 1431 (1987).
[7] E. Steigmeier and G. Harbeke, Solid State Commun. **8**, 1275 (1970).
[8] T. Matsunaga, H. Morita, R. Kojima, N. Yamada, K. Kifune, Y. Kubota, Y. Tabata, J.-J. Kim, M. Kobata, E. Ikenaga, and K. Kobayashi, J. Appl. Phys. **103**, 093511 (2008).
[9] K. M. Rabe and J. D. Joannopoulos, Phys. Rev. B **36**, 6631 (1987).
[10] M. Hase, M. Kitajima, S. Nakashima, and K. Mizoguchi, Appl. Phys. Lett. **83**, 4921 (2003).
[11] P. Fons, A. V. Kolobov, M. Krbal, J. Tominaga, K. S. Andrikopoulos, S. N. Yannopoulos, G. A. Voyiatzis, and T. Uruga, Phys. Rev. B **82**, 155209 (2010).
[12] A. Bussmann-Holder, H. Beige, and G. Völkel, Phys. Rev. B **79**, 184111 (2009).
[13] J. Hlinka, T. Ostapchuk, D. Nuzhnyy, J. Petzelt, P. Kužel, C. Kadlec, P. Vaněk, I. Ponomareva, and L. Bellaiche, Phys. Rev. Lett. **101**, 167402 (2008).
[14] W. Jantsch, H. Mitter, and A. Lopez-Otero, Z. Phys. B **41**, 287 (1981).
[15] A. Dreyhaupt, S. Winnerl, T. Dekorsy, and M. Helm, Appl. Phys. Lett. **86**, 121114 (2005).
[16] C. Kadlec, F. Kadlec, H. Němec, P. Kužel, J. Schubert, and G. Panaitov, J. Phys.: Condens. Matter **21**, 115902 (2009).
[17] L. Duvillaret, F. Garet, and J.-L. Coutaz, IEEE J. Sel. Top. Quantum Electron. **2**, 739 (1996).
[18] P. Kužel, H. Němec, F. Kadlec, and C. Kadlec, Opt. Express **18**, 15338 (2010).

[19]J. Petzelt, P. Kužel, I. Rychetský, A. Pashkin, and T. Ostapchuk, Ferroelectrics **288**, 169 (2003).
[20]T. Siegrist, P. Jost, H. Volker, M. Woda, P. Merkelbach, C. Schlockermann, and M. Wuttig, Nat. Mater. **10**, 202 (2011).
[21]R. Shaltaf, E. Durgun, J.-Y. Raty, P. Ghosez, and X. Gonze, Phys. Rev. B **78**, 205203 (2008).
[22]T. Matsunaga and N. Yamada, Phys. Rev. B **69**, 104111 (2004).
[23]A. H. Edwards, A. C. Pineda, P. A. Schultz, M. G. Martin, A. P. Thompson, H. P. Hjalmarson, and C. J. Umrigar, Phys. Rev. B **73**, 045210 (2006).
[24]L. Fekete, P. Kužel, H. Němec, F. Kadlec, A. Dejneka, J. Stuchlik, and A. Fejfar, Phys. Rev. B **79**, 115306 (2009).
[25]J. C. Dyre, J. Appl. Phys. **64**, 2456 (1988).
[26]I. Sakellis, Appl. Phys. Lett. **98**, 072904 (2011).